



AUTOMATIC DETECTION AND CLASSIFICATION OF DENTAL RESTORATIONS IN PANORAMIC RADIOGRAPHS

Talia Yeshua*	Jerusalem College of Technology, Jerusalem, Israel	tyeshua@gmail.com
Ya'akov Mandelbaum	Jerusalem College of Technology, Jerusalem, Israel	yaqovm@gmail.com
Ragda Abdalla-Aslan	Hebrew University Hadassah School of Dental Medicine, Jerusalem & Rambam Health Care Campus, Haifa, Israel	ragdaa@gmail.com
Chen Nadler	Hebrew University Hadassah School of Dental Medicine, Jerusalem, Israel	nadler@hadassah.org.il
Laureen Cohen	Jerusalem College of Technology, Jerusalem, Israel	laureenhoba@hotmail.fr
Levana Zemour	Jerusalem College of Technology, Jerusalem, Israel	levanazemour@hotmail.fr
Daniel Kabla	Jerusalem College of Technology, Jerusalem, Israel	eldanik1996@gmail.com
Ori Gleisner	Jerusalem College of Technology, Jerusalem, Israel	gleisner@g.jct.ac.il
Isaac Leichter	Jerusalem College of Technology, Jerusalem, Israel	leichter@jct.ac.il

* Corresponding author

ABSTRACT

Aim/Purpose	The aim of this study was to develop a prototype of an information-generating computer tool designed to automatically map the dental restorations in a panoramic radiograph.
Background	A panoramic radiograph is an external dental radiograph of the oro-maxillofacial region, obtained with minimal discomfort and significantly lower radiation dose compared to full mouth intra-oral radiographs or cone-beam computed tomogra-

Accepting Editor: Eli Cohen | Received: February, 4, 2019 | Revised: March 19, April 2, 2019 |
Accepted: April 7, 2019

Cite as: Yeshua, T., Mandelbaum, Y., Abdalla-Aslan, R., Nadler, C., Cohen, L., Zemour, L., ... Leichter, I.
(2019). Automatic detection and classification of dental restorations in panoramic radiographs. *Issues in Informing Science and Information Technology*, 16, 221-234. <https://doi.org/10.28945/4306>

(CC BY-NC 4.0) This article is licensed to you under a [Creative Commons Attribution-NonCommercial 4.0 International License](https://creativecommons.org/licenses/by-nc/4.0/). When you copy and redistribute this paper in full or in part, you need to provide proper attribution to it to ensure that others can later locate this work (and to ensure that others do not accuse you of plagiarism). You may (and we encourage you to) adapt, remix, transform, and build upon the material for any non-commercial purposes. This license does not permit you to use this material for commercial purposes.

phy (CBCT) imaging. Currently, however, a radiologic informative report is not regularly designed for a panoramic radiograph, and the referring doctor needs to interpret the panoramic radiograph manually, according to his own judgment.

Methodology	An algorithm, based on techniques of computer vision and machine learning, was developed to automatically detect and classify dental restorations in a panoramic radiograph, such as fillings, crowns, root canal treatments and implants. An experienced dentist evaluated 63 panoramic anonymized images and marked on them, manually, 316 various restorations. The images were automatically cropped to obtain a region of interest (ROI) containing only the upper and lower alveolar ridges. The algorithm automatically segmented the restorations using a local adaptive threshold. In order to improve detection of the dental restorations, morphological operations such as opening, closing and hole-filling were employed. Since each restoration is characterized by a unique shape and unique gray level distribution, 20 numerical features describing the contour and the texture were extracted in order to classify the restorations. Twenty-two different machine learning models were evaluated, using a cross-validation approach, to automatically classify the dental restorations into 9 categories.
Contribution	The computer tool will provide automatic detection and classification of dental restorations, as an initial step toward automatic detection of oral pathologies in a panoramic radiograph. The use of this algorithm will aid in generating a radiologic report which includes all the information required to improve patient management and treatment outcome.
Findings	The automatic cropping of the ROI in the panoramic radiographs, in order to include only the alveolar ridges, was successful in 97% of the cases. The developed algorithm for detection and classification of the dental restorations correctly detected 95% of the restorations. 'Weighted k-NN' was the machine-learning model that yielded the best classification rate of the dental restorations - 92%.
Impact on Society	Information that will be extracted automatically from the panoramic image will provide a reliable, reproducible radiographic report, currently unavailable, which will assist the clinician as well as improve patients' reliance on the diagnosis.
Future Research	The algorithm for automatic detection and classification of dental restorations in panoramic imaging must be trained on a larger dataset to improve the results. This algorithm will then be used as a preliminary stage for automatically detecting incidental oral pathologies exhibited in the panoramic images.
Keywords	medical information, panoramic images, dental restorations, radiologic informative report, machine learning, computer vision, image processing

INTRODUCTION

Many patients are apprehensive about dental treatments: their confidence in the dentist's diagnosis is low, and as a result they avoid preventive treatment in the early stage of the dental disease when damage is still minimal (Vassend, 1993). Dental imaging provides valuable information for diagnosis and treatment planning, which is not available through clinical examination or patient history (White et al., 2001). Information that can be extracted immediately by computer processing of the panoramic images and then conveyed directly to the patient would increase the patient's confidence in the doctor's diagnosis.

Imaging methods of the oro-maxillofacial region can be divided into intra-oral and extra-oral imaging. Extra-oral imaging are further classified into two-dimensional (Panoramic) and three-dimensional (Cone-Beam Computerized Tomography – CBCT) imaging (Guttenberg, 2008). Panoramic imaging is a two-dimensional image which demonstrates oro-maxillofacial hard tissues as well as soft tissue calcification, from the thyroid region up until the inferior border of the orbit and from one transverse vertebral process to the contra-lateral side (Huang, Klette, & Scheibe, 2008). Panoramic imaging is a tomography, where a specific pre-determined plane is clearly demonstrated, while other hard tissue structures are often blurred and superimposed at various levels. The panoramic image is a complex projection of the mandibular bones and their surrounding structure with multiple superimpositions and distortions which may be exacerbated by technical errors in image acquisition (Perschbacher, 2012).

Oro-maxillofacial imaging is prescribed by general dentists and dental specialists including orthodontists, prosthodontists, oral medicine specialists, and oral surgeons. The indications for panoramic image are diverse and include developmental assessment, impacted teeth, bone pathologies, trauma, salivary gland pathology, and general review prior to dental treatment plan. The limitations of the panoramic image include geometric distortion, locally varying noise levels, low contrast, asymmetry, superimposition of bony structures (such as the spine or the contralateral jaw) as well as airways, and overlap of adjacent teeth, which may be aggravated by faulty positioning of the patient (Wanat & Frejlichowski, 2011). Nevertheless, panoramic imaging is an excellent choice for the clinician, due to its broad demonstration of most of the oro-maxillofacial structures, with minimal patient discomfort, compared to a full-mouth-series of intraoral radiographs. Most importantly, the radiation dose in panoramic imaging (14.2-24.3 microSv) is significantly lower compared to the radiation dose involved in a full-mouth-series of intra-oral radiographs (34.9-170.7 microSv) (Ludlow, Davies-Ludlow, & White, 2008) or in a maxillo-mandibular CT scan (2100 microSv) (Ngan, Kharbanda, Geenty, & Darendeliler, 2003).

The panoramic radiograph includes essential and comprehensive information regarding oral pathologies and dental restorations such as fillings, root canal treatments, implants, and crowns. In contrast to ordinary medical radiology, in oro-maxillofacial imaging the referring doctor is also the one in charge of the image's interpretation, as images are typically generated in an imaging clinic which does not employ a radiologist. Thus currently, there is no common practice of composing a radiographic report for panoramic images, which is essential for follow-up of misdiagnoses by the interpreting doctor (Delai et al., 2015). Automatic detection and classification of the dental restorations is an initial stage for enabling detection of oral pathologies such as caries and inflammation which are often formed adjacent to an existing dental restoration. In addition, this stage is required in order to map the dental restorations in the oral cavity and separate them from the rest of the findings that will be characterized in later stages of the study.

An algorithm for the early detection of oral pathologic findings on panoramic radiographs was not reported in the literature. Most of the studies dealing with computerized processing of dental panoramic radiographs refer to the development of algorithms which identify the teeth only, without detecting dental restorations. A tooth segmentation technique for panoramic images, based on a wavelet transformation, was proposed (Patanachai, Covavisaruch, & Sinthanayothin, 2010). Poonsri, Aimjirakul, Charoenpong, and Sukjamsri (2016) proposed a fully automatic algorithm to segment the teeth, which consists of three steps: tooth area identification, template matching of single and double rooted teeth, and tooth area segmentation. The accuracy of their algorithms was less than 50%, due to tooth inclination and due to low image contrast between the teeth and the gum. Lira, Giraldo, Neves, and Feijoo (2014) proposed a segmentation approach based on supervised learning techniques for texture recognition. A Bayesian classifier could distinguish between pixels inside the teeth and pixels outside the teeth, but this algorithm was applied only to four panoramic radiographs with an accuracy of 81.3% (Lira et al., 2014). An algorithm developed to detect wisdom teeth only, using basic functions of image processing, as well as the relative order in which these teeth appear in the panoramic

radiograph, was presented (Amer & Aqel, 2015). An algorithm for segmentation and for characterization of teeth with and without caries was described (Oliviera & Proença, 2011), but this algorithm does not detect the precise location of the caries.

MATERIALS AND METHODS

Sixty-three panoramic images with 316 dental restorations were evaluated. The panoramic images were anonymized and each image was assigned a study number. An experienced dentist evaluated the images and marked manually on each image all the existing dental restorations, which were classified into nine categories (See Table 1). Figure 1 shows an example of the dentist's annotations on the panoramic image.

Table 1. Division of dental restorations into categories

Group number	Type of Restoration	Acronyms
1	Crown (only)	CRW
2	Root Canal Treatment with Core	RCT-CO
3	Root Canal Treatment with Core & Crown	RCT-CO-CRW
4	Dental Implant (only)	DI
5	Dental Implant with Abutment	DI-A
6	Dental Implant with Crown	DI-CRW
7	Amalgam Filling	AF
8	Composite Filling	CF
9	Connected Restorations	MULTI

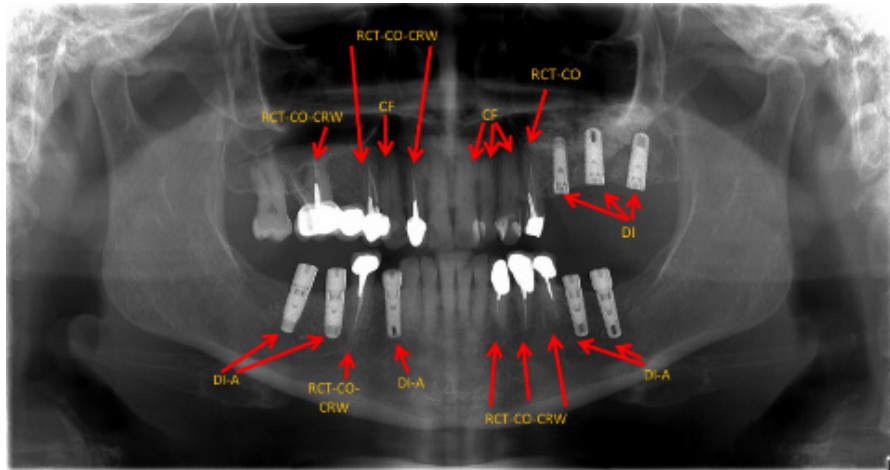


Figure 1. A panoramic image including dentist's annotations specifying dental restorations

THE AUTOMATIC DETECTION STAGE

Automatic cropping of the region of interest

The purpose of the algorithm which was developed was to automatically detect and classify all the dental restorations in the panoramic images at an accuracy level comparable to the manual assessment of the experienced dentist. First, the dental restorations should be accurately detected and then they have to be correctly classified into the different categories, which are displayed in Table 1. The algorithm was developed in the Matlab programming environment. Since the dental restorations are located only in the alveolar ridge region in the panoramic image, the first stage of the algorithm was to automatically crop this region of interest from the panoramic image. Although the panoramic images which were evaluated had different spatial resolutions, the location of the alveolar ridge area in the image was generally uniform, so an equal crop in relative values of the length and the width of the image could be performed. Various values of the latter were examined in order to obtain an optimal region of interest. The location of the crop in the vertical axis was set so that the upper limit of the region of interest was 18% lower than the upper border of the image, while the lower limit was set to be 24% higher than the lower border of the image. On the horizontal axis, the region of interest was cropped symmetrically - 17% on both sides of the image. Figure 2 shows an example of an automatically cropped panoramic image.

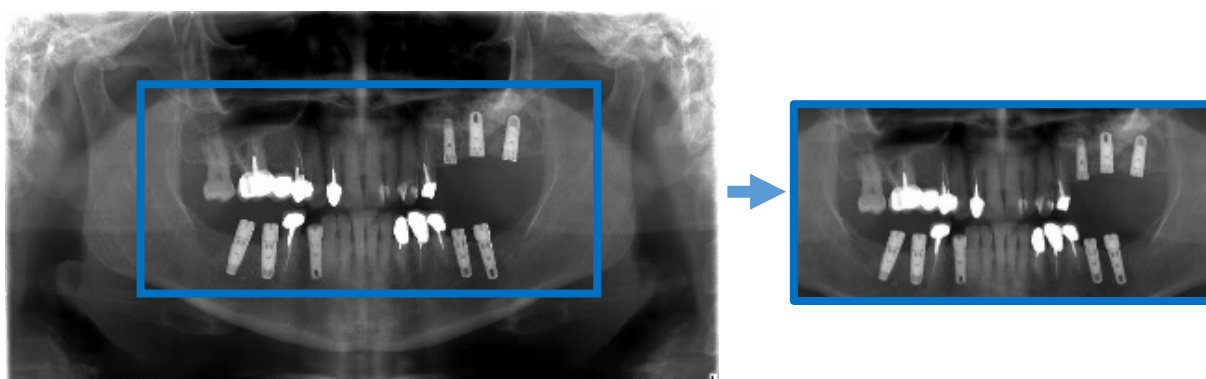


Figure 2. Automatic cropping of the region of interest

Automatic segmentation of the dental restorations

In the field of computer vision, object segmentation is used in order to detect specific objects in an image. The goal of segmentation is to automatically locate objects and boundaries in the image. More precisely, image segmentation is the process of assigning a label to every pixel in an image such that pixels with the same label can be considered to belong to the same object. Our goal was to label the pixels belonging to the various dental restorations, within the region of interest that was automatically cropped from the panoramic image. The panoramic image is a grayscale image, composed of different shades of gray known as gray level values, so that pixels with low values represent dark areas and pixels with high values represent bright areas. Since typical restorations appear brighter in the image than their surroundings, their pixels have higher gray level values than pixels that belong to teeth and other tissues appearing in the image. Therefore, segmentation was performed by calculating a gray level threshold, which separates the pixels in the image into two classes. The foreground pixels – those belonging to the dental restorations – have gray level values higher than the threshold, while background pixels, which belong to the surrounding tissues have gray levels lower than the threshold. Since the brightness of the panoramic image is not spatially homogeneous, a single global threshold value was not suitable for the entire image. Instead, an adaptive approach was required, making use of different threshold values in different regions of the image.

The adaptive thresholding method calculates a matrix of threshold values, assigning each pixel in the image its own threshold value. If the gray level of the pixel is higher than the threshold value, it will be considered as a pixel that belongs to the foreground – i.e., a dental restoration. The threshold value for each pixel in the image is calculated by using a ‘pixel-neighborhood matrix’, which is a matrix of gray level values of pixels located in the vicinity of the pixel under study. The default size of the neighborhood matrix, used by the algorithm, is one eighth of the image height and one eighth of its width. Based on experimentation, it was decided not to assign a uniform weight to all the pixels in the neighborhood matrix, for the purpose of calculating the threshold value. The best results were obtained using a Gaussian filter that weights the pixels in accordance with a Gaussian bell-curve centered on the pixel of interest. This means that gray level values of pixels that are located far from the central pixel have a lower weight in the calculation of the threshold value of the pixel. Figure 3A shows an example of segmentation using the Gaussian filter calculation.

Several morphological operations were required to improve the results of the initial segmentation by the adaptive threshold. Morphological operations are a set of image processing tools which adjust the shapes of the objects. In a morphological operation, each pixel in the image is adjusted, based on whether or not foreground pixels are contained within its neighborhood. In the first stage, a morphological opening was performed to separate adjacent restorations that were erroneously identified as a single segmented region. The opening operation removes small objects from the foreground of the image and associates them with the background. The size and shape of the objects removed depend on the structuring element which is selected for this purpose. Regions of the foreground into which the structuring element cannot fit without protruding out in the background, such as corners and narrow connecting regions, will be removed and included in the background of the image. Following several trials, a rectangular structuring element, 10 pixels wide and 3 pixels high, was selected. Since this operation also tends to create “holes”, disconnecting regions that ought properly to be considered as a single segmented region, a closing operation was then performed. Dual to the opening operation, a closing operation essentially performs an opening on the background. Thus it removes small objects from the background of the image (small holes) and places them in the foreground. The structuring element that was used for the closing operation was a minimal square, of 3x3 pixels. At this stage, the foreground of the image also included segmented regions smaller than the size of a standard dental restoration. Therefore, in the following step the algorithm removed all the segmented regions containing less than 450 pixels. Finally, an internal-hole-filling operation was performed in order to include in the segmented region all internal pixels that were not marked as foreground pixels. Figure 3B shows the results of the algorithm after carrying out the morphological operations.

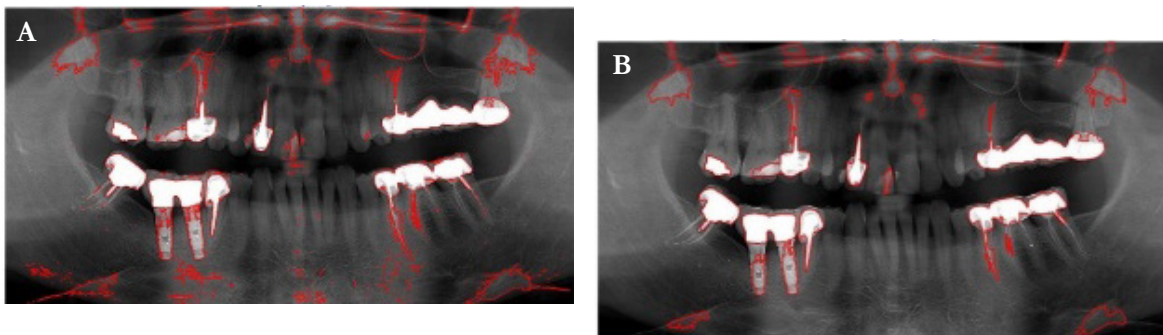


Figure 3. Segmentation of dental restorations using the Adaptive Threshold method.

A. Initial segmentation results using Gaussian filter calculation.

B. Segmentation results following morphological operations.

Improving the detection by optimizing the segmentation process

In order to improve the detection rate of dental restorations the segmentation process was next optimized by adjusting the parameters of the adaptive threshold. The first parameter to be adjusted was the “sensitivity level”, which determines the percentile cut-off for gray level values that are defined as belonging to foreground pixels. As the sensitivity level increases, the threshold value decreases and more pixels are included in the segmented region. The threshold value was set at 0.2, which means that the threshold is determined as the 80th percentile of the local gray level distribution in the neighboring pixel matrix.

Figure 4 displays the segmentation results using a sensitivity level of 0.3 (Figure 4A) in comparison with the results obtained by using a sensitivity level of 0.2 (Figure 4B). The arrows in Figure 4A indicate the segmented areas that were erroneously added to the dental restorations, using a sensitivity level of 0.3. Figure 4B shows that these errors were corrected by using a sensitivity level of 0.2, and the accuracy of the segmentation was improved. In addition, when this sensitivity level was applied, a few regions not containing dental restorations were erroneously detected as such (false-positive detection). It should be noted that at this stage of optimization, the segmentation resulted in some dental restorations that were detected as such, but with a boundary deviating from the correct boundary, as exemplified by the green arrow in Figure 4B.

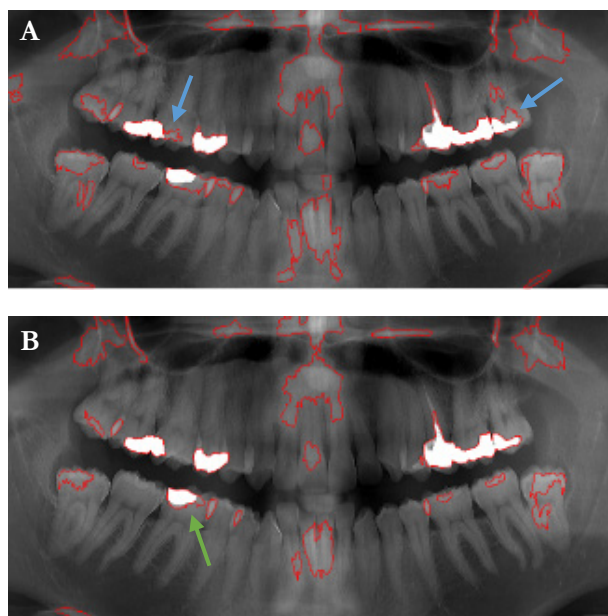


Figure 4. The effect of modifying the sensitivity level on the segmentation results.

A. Segmentation results for a sensitivity level of 0.3.

B. Segmentation results for a sensitivity level 0.2.

In order to identify the boundary of the detected dental restoration more accurately, the adaptive thresholding process was improved by modifying another parameter – the size of the pixel-neighborhood matrix. For this purpose, neighborhood-matrices of several sizes were examined and it was found that a neighborhood-matrix of size 101 x 51 pixels (width x height) yielded optimal results. Figure 5A demonstrates the segmentation results with a matrix of size 201 x 51 pixels and Figure 5B shows the segmentation results using a pixel-neighborhood matrix of size 101 x 51 pixels. The arrows in Figure 5A indicate segmentation errors where the matrix width is too large (201 pixels), which were corrected when the neighbor matrix was selected to have width of 101 pixels.

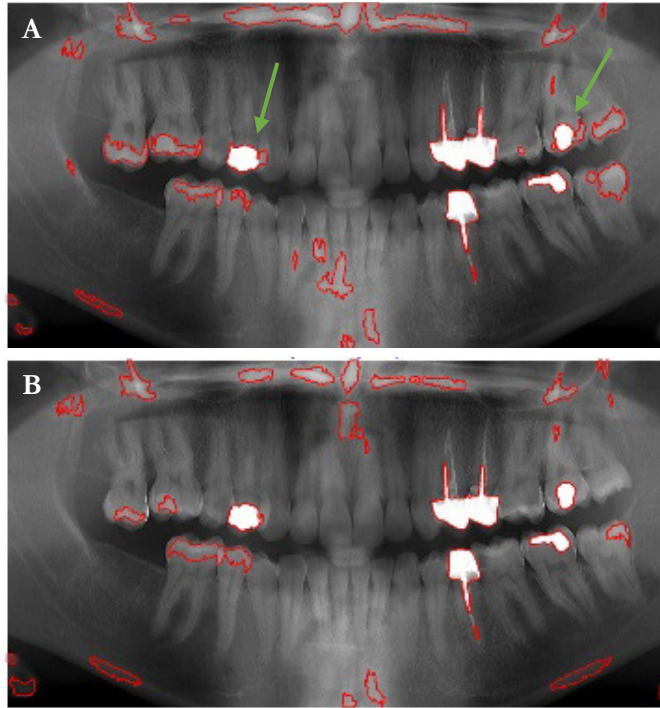


Figure 5. The effect of modifying the size of the pixel neighbor-matrix.

A. Segmentation results using a matrix of size 201 x 51 pixels.

B. Segmentation results using a matrix of size 101 x 51 pixels.

Another challenge which arose was the relatively high rate of false positive detection, i.e., regions that were erroneously detected as dental restorations. To reduce this number of incorrectly segmented regions, the algorithm removed all the components which were deemed close to the borders of the image. We found that regions whose center of mass is located in the top 15% of the image and in the bottom 12% of the image do not represent restoration and therefore should not be considered as dental restorations. Figure 6 illustrates the results of the removal of these regions from the set of detected restorations.

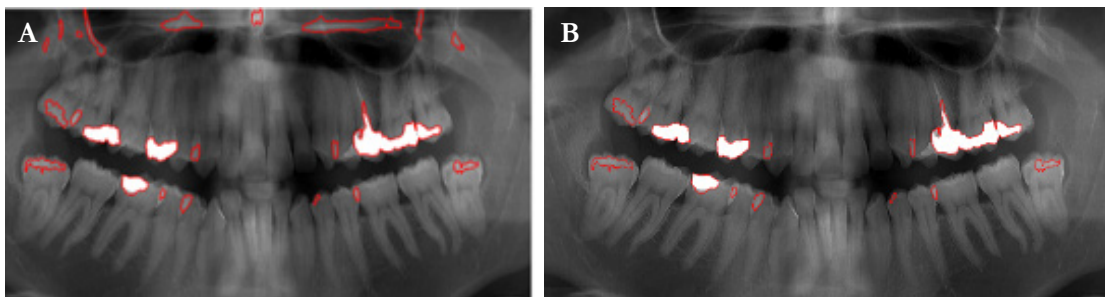


Figure 6. Removal of regions adjacent to image borders.

A. Segmentation results before removing the regions close to image borders.

B. Segmentation results after removing these regions.

Though the problem of the false detections near the image borders was resolved, there still remained regions which were erroneously segmented as restorations because they were brighter than their surroundings. A total of 528 different regions were detected, 228 falsely. The latter group of regions was divided into three categories:

- Regions of apparent overlap between neighboring teeth, which appear brighter than their surroundings.
- Tooth enamel, which often appears brighter than its surroundings.
- Other errors in detection.

The goal in the following phase was to categorize each segmented region, and remove regions identified as belonging to these categories. The overall false positive rate could thus be improved.

THE AUTOMATIC CLASSIFICATION STAGE

In the classification phase, a set of 12 categories was defined, including the nine dental restorations categories and the three false categories mentioned above. The classification algorithms learn the unique characteristics of each group, using a set of segmented regions as a training data, and build models for classification. Using these classification models, each new segmented region was automatically classified as belonging to one of the 12 categories, and the results of the classification were compared to the manual estimation of the dentist. The classification of the various dental restorations was carried out using shape and texture characteristics of the detected regions. The restorations differ from each other, both in their shape and in the distribution of gray levels within the restoration. For example, the shape of a normal dental filling is markedly different from that of a root canal or implant. In terms of the texture of the interior region, composite fillings contain darker pixels than amalgam fillings, even though they are similar in shape.

The algorithm classified each detected structure using twenty numerical features. These include eight shape characteristics such as the area (the number of pixels contained in the structure), the perimeter, the area-equivalent-diameter (diameter of the circle of same area), and the solidity (the ratio of the area of the region to the area of the convex hull). Seven of the features are texture characteristics computed using the gray level values of the pixels in the interior of the region, including the average gray level, the standard deviation of the gray level, the contrast and the statistical entropy. Five additional texture properties, such as the entropy, homogeneity, and the energy, were computed using the Gray Level Co-occurrence Matrix (GLCM), which is the bivariate distribution for pairs of gray levels appearing side-by-side. This improves upon the global distribution, since it also takes into account the spatial allocation of gray levels.

All the 528 detected regions were used for training the software. Twenty-two different classification algorithms were evaluated. These algorithms included Decision Trees, Support Vector Machines (SVM), and K-Nearest Neighbors (KNN) and variations.

Since the number of panoramic images included in the study (63) was relatively small, the method of cross-validation was applied to evaluate the classification success rate of the various models. To this end, the 528 regions were randomly divided into 5 groups. Training was carried out using four groups from the database while classification was tested using the fifth group. This was repeated five times, varying the test group and training groups appropriately each time. The results were compared to the known classification tags of each group. The model found to give the best predictive results is Weighted k-NN. Like ordinary k-NN, this model takes a membership vote amongst the k training samples nearest the candidate, but weights the vote, assigning higher weight to nearby samples. The category chosen, v_0 , is that which gets the largest vote, calculated according to

$$D(x_q, v_0) = \sum_{i=1}^k w_i \delta_{v_0, v(x_i)}$$

where x_q is the feature vector under study, v_0 is the index of the category, $\{x_i\}_{i=1..k}$ are the k nearest neighbors, $v(x_i)$ is the category to which each of the latter belongs, and $\delta_{m,n}$ is the Kronecker delta. The weights w_i are taken to be the inverse square of the distance:

$$w_i = \frac{1}{d(x_q, x_i)^2}$$

RESULTS

The automatic method for cropping the alveolar region yielded satisfactory results in 97% of the cases (61 of the 63 panoramic images), while two images were cropped manually.

In order to evaluate the quality of the segmentation for the 5 types of restorations present in the images, the percentage of structures that were correctly segmented following all phases of improvement and optimization was determined visually. Figure 7 summarizes the segmentation success rate for the detection of the different types of dental restorations. It should be noted that in the results concerning the segmentation phase there are only 5 categories of restorations, although in the classification phase there are 9 categories. This is due to the fact that for in the segmentation phase the pixels of a crown (CRW), for example, should be segmented independently of the sub-categories (CRW, DI-CRW or RCT-CO-CRW) since they have similar gray levels and similar surrounding pixels. However, in the classification phase of the algorithm, they should be classified into the 3 different categories.

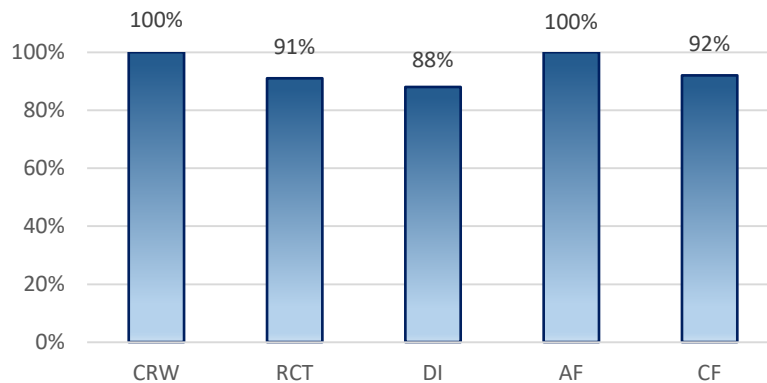


Figure 7. Success rate of detection for various categories of restorations.

Figure 7 shows that the crowns and amalgam fillings were detected with 100% success. Segmentation of the composite fillings was more complex, because their gray level is lower than the other restorations. Root canal treatments were sometimes difficult to detect due to their narrow structure. The lowest success rate of the segmentation occurred for the implants (88%), both because the gray level of the implant is lower than the other restorations, and also because their structure is more complex. In general, the algorithm automatically detected 95% of the existing restorations in the panoramic-images in the dataset.

Using the Weighted k-NN classification model, the correct classification rate was 92%. Other models such as "Cubic SVM" and "Quadratic SVM" achieved lower success rates – 87% and 84%, respectively. Figure 8 shows the success rate of the classification of the detected regions into the different categories using the Weighted K-NN model. This figure shows that some categories, such as crowns and implants, were readily identified, while others were somewhat more challenging to classify.

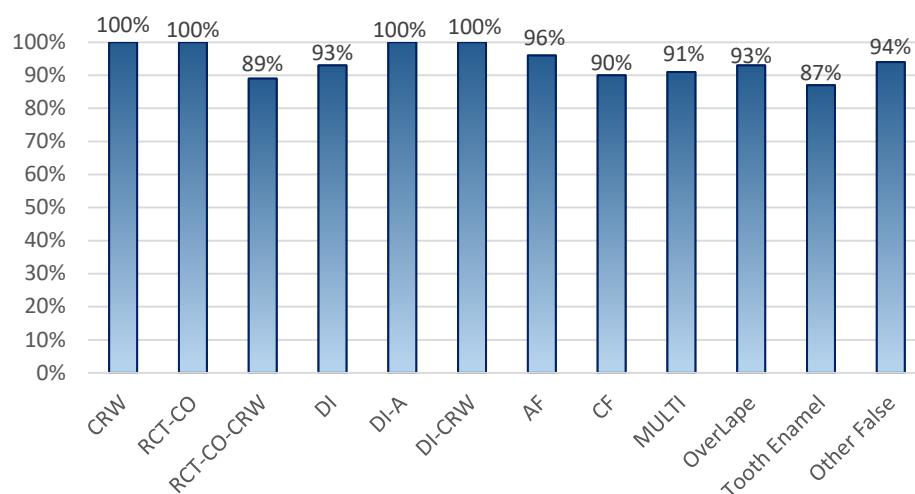


Figure 8. Classification success rate using Weighted K-NN model.

As alluded to above, the classification categories included three types of segmented regions that are not dental restorations. The rate of undesirable (false positive) segmented regions was examined following the classification stage. It was found that of the 228 undesirable segmented regions, 223 regions were categorized as false detections and only five were incorrectly classified as dental restorations. Since 98% of the undesirable regions were eventually removed from consideration, on average there were only 0.08 false marks per image. On the other hand, of the 316 dental restorations that were marked manually by the dentist, 300 were automatically segmented by the algorithm and 293 were correctly categorized as restorations. Only seven were incorrectly identified as superfluous regions (false negatives). This represents an automatic detection of the dental restorations with a success rate of 93%.

CONCLUSION

In this study, we have shown that it is possible to automatically detect the dental restorations in panoramic images, using tools of image processing, computer vision and machine learning. The success of the segmentation of the dental restorations ranged from 88% to 100%, depending on the type of restoration. The total success rate of the classification algorithm was 92%. To improve segmentation, the inclusion of additional, contour-based recognition methods, as well as the application of the much-heralded 'Deep Learning' classifiers, which are not based on segmentation, is planned in the future. Increasing the training image dataset will further increase the accuracy of classification. Augmenting the image dataset will also facilitate the next phase – the detection of pathologies in the oral cavity – where the use of the methods described is also planned. The automatic detection and classification of dental restorations, and in pursuing stages, identification of pathologies as well, will assist the dentist in decision-making and treatment planning. This information, produced automatically and provided immediately following the panoramic imaging, will help form the basis for a radiologic report, which is currently unavailable, will increase the patient's confidence in the clinician's diagnosis and encourage acceptance of the proposed treatment plan.

REFERENCES

- Amer, Y. Y., & Aqel, M. J. (2015). An efficient segmentation algorithm for panoramic dental images. *Procedia Computer Science*, 65, 718-725. <https://doi.org/10.1016/j.procs.2015.09.016>

Mapping Dental Restorations in Panoramic Radiographs

- Delai, D., Bernardi, A., Felipe, G. S., da Silveira Teixeira, C., Felipe, W. T., & Felipe, M. C. S. (2015). Florid cemento-osseous dysplasia: A case of misdiagnosis. *Journal of Endodontics*, 41(11), 1923-1926. <https://doi.org/10.1016/j.joen.2015.08.016>
- Guttenberg, S. A. (2008). Oral and maxillofacial pathology in three dimensions. *Dental Clinics of North America*, 52(4), 843-873. <https://doi.org/10.1016/j.cden.2008.06.004>
- Huang, F., Klette, R., & Scheibe, K. (2008). *Panoramic imaging: Sensor-line cameras and laser range-finders*. Singapore: John Wiley & Sons Press. <https://doi.org/10.1002/9780470998267>
- Lira, P. H. M., Giraldo, G. A., Neves, L. A. P., & Feijoo, R. A. (2014). Dental r-ray image segmentation using texture recognition. *IEEE Latin America Transactions*, 12(4), 694-698. <https://doi.org/10.1109/TLA.2014.6868871>
- Ludlow, J. B., Davies-Ludlow, L. E., & White, S. C. (2008). Patient risk related to common dental radiographic examinations: The impact of 2007 International Commission on Radiological Protection recommendations regarding dose calculation. *The Journal of the American Dental Association*, 139(9), 1237-1243. <https://doi.org/10.14219/jada.archive.2008.0339>
- Ngan, D., Kharbanda, O. P., Geenty, J. P., & Darendeliler, M. (2003). Comparison of radiation levels from computed tomography and conventional dental radiographs. *Australian Orthodontic Journal*, 19 (2), 67.
- Oliveira, J., & Proença, H. (2011). Caries detection in panoramic dental X-ray Images. In J Tavares & R. N. Jorge (Eds.), *Computational Vision and Medical Image Processing* (pp. 175-190). Dordrecht: Springer Press. https://doi.org/10.1007/978-94-007-0011-6_10
- Patanachai, N., Covavisaruch, N., & Sinthanayothin, C. (2010). Wavelet transformation for dental X-ray radiographs segmentation technique. *International Conference on ICT and Knowledge Engineering*. <https://doi.org/10.1109/ictke.2010.5692904>
- Perschbacher, S. (2012). Interpretation of panoramic radiographs. *Australian Dental Journal*, 57, 40-45. <https://doi.org/10.1111/j.1834-7819.2011.01655.x>
- Poonsri, A., Aimjirakul, N., Charoenpong, T., & Sukjamsri, C. (2016). Teeth segmentation from dental x-ray image by template matching. *Biomedical Engineering International Conference (BMEiCON)*. <https://doi.org/10.1109/bmeicon.2016.7859599>
- Vassend O. (1993) Anxiety, pain and discomfort associated with dental treatment. *Behaviour Research and Therapy*, 31(7), 659-666. [https://doi.org/10.1016/0005-7967\(93\)90119-f](https://doi.org/10.1016/0005-7967(93)90119-f)
- Wanat, R., & Frejlichowski, D. (2011). A problem of automatic segmentation of digital dental panoramic x-ray images for forensic human identification. In *15th Central European Seminar on Computer Graphics (CESCG 2011)*.
- White, S. C., Heslop, E. W., Hollender, L. G., Mosier, K. M., Ruprecht, A., & Shrout, M. K. (2001). Parameters of radiologic care: An official report of the American Academy of Oral and Maxillofacial Radiology. *Oral Surgery, Oral Medicine, Oral Pathology, Oral Radiology, and Endodontology*, 91(5), 498-511. <https://doi.org/10.1067/moe.2001.114380>

BIOGRAPHIES



Dr. Talia Yeshua holds a Ph.D. in applied physics from the Hebrew University of Jerusalem. Her doctoral dissertation involved an interdisciplinary research in the field of nanoprinting and nanoelectronics. She is a lecturer in the Department of Applied Physics/Electro-Optics Engineering at the Jerusalem College of Technology. Her research focus is on computerized diagnosis of various pathologies in medical images, using computer vision and machine learning tools.



Ya'akov Mandelbaum studied Mathematics and Physics at the undergraduate and graduate levels at the University of Pennsylvania, MIT, and the Hebrew University of Jerusalem. After working in industry as a Physicist and Electro-Optics team leader, he joined the Lev Academic Center as a lecturer and researcher in the Department of Applied Physics and Electro-Optics. In parallel, he is currently pursuing a PhD at Bar-Ilan University.



Ragda Abdalla-Aslan is an oral medicine specialist in the Department of Oral medicine, Sedation and Maxillofacial Imaging, Hebrew University-Hadassah school of dental medicine, Jerusalem, Israel and an attending physician at the department of oral and maxillofacial surgery, Rambam Health Care Campus, Haifa, Israel. She had been involved in research, has peer-reviewed publications, regularly reviews manuscripts for journals spanning oral medicine and dentistry, and won several scholarships and awards. She is a board member of the maxillofacial radiology committee of the Israeli Association of Oral Medicine.



Dr. Chen Nadler is an Oral Medicine Specialist (DMD PhD), who's main practice area is oro-maxillofacial imaging. Currently. She is the head of the Oral Maxillofacial Imaging Unit, in the Faculty of Dentistry, at Hadassah Medical School. In charge of teaching, research and service in the field of oro-maxillofacial imaging. She did her one-year sub-training at the University of Toronto in the Oral Radiology department. Her main research interests are: image analysis, salivary gland imaging, bone lesions interpretation and optimal imaging as well as educational research.



Lauren Cohen completed her undergraduate studies in Computer Science Engineering at the Jerusalem College of Technology. Her research involves development of algorithms for detecting pathologies in medical images using advanced image processing and machine learning tools.



Levana Zemour completed her undergraduate studies in Computer Science Engineering at the Jerusalem College of Technology. Her research involves development of algorithms for detecting pathologies in medical images using advanced image processing and machine learning tools.



Daniel Kabla is finishing his studies for a bachelor degree in Electrical Engineering, at the Jerusalem College of Technology, Jerusalem, Israel. In the last year of his studies he joined the Image Processing research team in the Medical Optics Laboratory at the college. He is interested also in modern communication and acoustic communication under water.



Ori Gleisner received his B.Sc. degree in Electro-optics Engineering, at the Jerusalem College of Technology, and his M.Sc. degree in Optoelectronics and Photonics Engineering at the Ben-Gurion University of the Negev, Israel. In recent years he is active as a member of the research team developing algorithms for processing medical images in the Medical-Optics Laboratory at the Jerusalem College of Technology.



Prof. Leichter holds a Ph.D. from the Hebrew University of Jerusalem. He specialized in medical physics and medical engineering at UCLA and the Hebrew University. He is a Full Professor in the Department of Applied Physics/Electro-Optics Engineering and head of the Medical Optics Laboratory at the Jerusalem College of Technology.